Contribution from the Department of Chemistry,
Texas A&M University, College Station, Texas 77843

Ligand-Centered Oxidation of Manganese(II) Complexes

Silvia A. Richert, Paul K. S. Tsang, and Donald T. Sawyer*

Received October 14, 1987

The oxidation potentials for an extensive group of manganese(II) complexes and their zinc(II) analogues have been determined by cyclic voltammetry in acetonitrile. With the exception of the pyridine, pyridine *N*-oxide, and H_2O ligands, the oxidations of the manganese(II) complexes occur at substantially less positive potentials than those for the zinc(II) analogues and clearly are ligand-centered. The removal of an electron from the valence shell of the ligand is easier than removal from the d^5 manifold of manganese(II) and is facilitated by formation of a manganese (d-electron)–ligand (p-electron) covalent bond. The negative shift in potential for ligand oxidation is proportional to the bond energy. The near-edge X-ray absorption energies for the oxidized and reduced forms of the manganese complexes have been determined and correlated with the electrochemical results. The edge energy for manganese(II) is 6546.0 ± 0.3 eV, for manganese(III), 6550.0 ± 0.5 eV, and for the manganese(II) covalently bonded to an oxidized ligand, 6548.3 ± 0.5 eV. A manganese(II/III) valence change has a shift of 4.0 eV, and the formation of a manganese(II)–(•L) covalent bond from a ligand-centered oxidation has an average shift of 2.3 eV per bond formed. Formulation of MnO_4^- as $Mn^{II}(^{\bullet}O^{\bullet})(^{\bullet}O^-)_3^-$ with five Mn–O covalent bonds leads to a predicted edge energy of 6557.5 eV; the observed value is 6556.5 eV.

There is increasing evidence that many transition-metal complexes have substantial covalent bond character.[1-4] This has important implications for oxidation–reduction catalysis by manganese proteins such as the oxygen-evolving complex[5-6] of photosystem II, the pseudocatalase of *Lactobacillus plantarum*,[7-9] and the mitochondrial superoxide dismutases.[10-15] The chemical mechanisms for the substrate transformations of these manganese proteins are not understood, but model studies often invoke the participation of a redox shuttle between the Mn(II) and Mn(III) valence states and in some cases the Mn(IV) or Mn(V) states.[7,8,16,17] The degree of covalency for manganese–oxygen bonds that is indicated from charge density considerations[1-4,18] precludes the presence of the electropositive center of high-valent manganese in biological complexes.

A recent X-ray crystallographic investigation[19] (to 2.4-Å resolution) of the manganese superoxide dismutase *Thermus thermophilus* demonstrates that the central manganese is bound by three histidines and one aspartic acid. Because the apparent function of this protein is to disproportionate superoxide into hydrogen peroxide and oxygen ($2O_2^{-\bullet} + 2HA \xrightarrow{E} H_2O_2 + O_2 + 2A^-$) via redox catalysis, the electron-transfer facilitation is assumed to be manganese-centered. However, the redox potentials and the presence of a carboxylate ligand indicate that a ligand-centered electron transfer is possible and needs to be considered. Such ligand-centered electron-transfer oxidation occurs in the bis(toluene-3,4-dithiolato) complexes of copper(II), nickel(II), cobalt(II), iron(II), and manganese(II).[20]

Although the electronic formulation of manganese(III) and manganese(IV) complexes has a long and extensive chemical tradition,[21] those that contain organic anionic ligands exhibit anomalous redox and ligand substitution behavior relative to that for analogous iron(III) complexes. Whereas the aqueous standard reduction potential for the Mn(III/II) couple (+1.51 V vs NHE) is 0.7 V more positive than that for the Fe(III/II) couple (+0.77 V), the reduction potential for the MnL_3 complex (L^- = 8-quinolinate) is only 0.3 V positive relative to that for the $Fe^{III}L_3$ complex. A more dramatic anomaly is the reduction potential of +0.06 V vs NHE for the $PMn(ClO_4)/PMn^{II}$ couple[22] versus +0.35 V for the $PFe^{III}(ClO_4)/PFe^{II}$ couple (P = tetraphenylporphinato dianion).[23] Also, most iron(III), iron(II), and manganese(II) complexes are labile to ligand substitution reactions, but MnL_3 complexes are inert. Because a recent theoretical analysis[1] for the d^5 Cr(I) ion [isoelectronic with the d^5 Mn(II) ion] concludes that the electron-density distribution for the CrO^+ ion is between d^5 and d^4 [$Cr^I(^{\bullet}O^{\bullet})^+ \leftrightarrow Cr^{II}(^{\bullet}O^-)^+$], the valence state for the more electronegative Mn(II) ion in the isoelectronic MnO^{2+} ion must be essentially d^5 [$Mn^{II}(^{\bullet}O^{\bullet})^{2+}$].

The electrochemical oxidation of a series of manganese(II) complexes has been investigated to gain insight to the mode and site of electron transfer and correlated with near-edge X-ray absorption energies for reduced and oxidized manganese complexes. Oxidation potentials, which depend on the oxidation state of the metal, the charge of the complex, the ligand, and the solvent, correlate with the initial site of electron transfer. X-ray absorption edge data provide a measure of the electron density at the metal center. The position of the edge is primarily dependent on valence, although other factors such as coordination number and geometry, type of bonding, and charge also influence the edge position. Taken together, these techniques provide an effective means to distinguish between ligand-centered and metal-centered oxidations of manganese(II) complexes. The proposition is that the removal of an electron from the valence shell of the ligand is easier than from the d^5 manifold of manganese(II) and is facilitated by formation of a manganese (d-electron)–ligand (p-electron) covalent bond.

$$Mn^{II}(L^-)_3^- \rightarrow Mn^{II}(^{\bullet}L)(L^-)_2 + e^- \qquad (1)$$

The negative shift in the potential for ligand oxidation (relative to that for the free ligand anion) is proportional to this covalent bond energy. This has been demonstrated for the bis(toluene-3,4-dithiolato) complexes of Cu(II), Ni(II), Co(II), Fe(II), and

(1) Harrison, J. F. *J. Phys. Chem.* **1986**, *90*, 3313.
(2) Sanderson, R. T. *Inorg. Chem.* **1986**, *25*, 3518.
(3) Di Bella, S.; Fragala, I.; Granozzi, G. *Inorg. Chem.* **1986**, *25*, 3997.
(4) Low, J. J.; Goddard, W. A., III. *J. Am. Chem. Soc.* **1986**, *108*, 6115.
(5) Cheniae, G. M.; Martin, I. F. *Biochim. Biophys. Acta* **1970**, *197*, 219.
(6) Heath, R. L. *Int. Rev. Cytol.* **1973**, *34*, 49.
(7) Kono, Y.; Fridovich, I. *J. Biol. Chem.* **1983**, *258*, 6015.
(8) Kono, Y.; Fridovich, I. *J. Biol. Chem.* **1983**, *258*, 13646.
(9) Beyer, W. F., Jr.; Fridovich, I. *Biochemistry* **1985**, *24*, 6460.
(10) Weisiger, R. A.; Fridovich, I. *J. Biol. Chem.* **1973**, *248*, 3582.
(11) Ravindranath, S. D.; Fridovich, I. *J. Biol. Chem.* **1975**, *250*, 6107.
(12) Asada, K.; Yoshikawa, K.; Takahashi, M.; Maeda, Y.; Enmanji, K. *J. Biol. Chem.* **1975**, *250*, 2801.
(13) Lumsden, J.; Cammack, R.; Hall, D. O. *Biochim. Biophys. Acta* **1976**, *438*, 380.
(14) Brock, C. J.; Harris, J. I.; Sato, S. *J. Mol. Biol.* **1976**, *107*, 175.
(15) Brock, C. J.; Harris, J. I. *Biochem. Soc. Trans.* **1977**, *5*, 1537.
(16) Dekker, J. P.; Van Gorkom, H. J.; Brok, M.; Ouwehand, L. *Biochim. Biophys. Acta* **1984**, *764*, 301.
(17) Cheniae, G. *Annu. Rev. Plant Physiol.* **1970**, *21*, 467.
(18) Sawyer, D. T. *Comments Inorg. Chem.* **1987**, *6*, 103.
(19) Stallings, W. C.; Pattridge, K. A.; Strong, R. K.; Ludwig, M. L. *J. Biol. Chem.* **1985**, *260*, 16424.
(20) Sawyer, D. T.; Srivatsa, G. S.; Bodini, M. E.; Schaefer, W. P.; Wing, R. M. *J. Am. Chem. Soc.* **1986**, *108*, 936.
(21) Yamaguchi, K. S.; Sawyer, D. T. *Isr. J. Chem.* **1985**, *25*, 164.
(22) Boucher, L. J.; Garber, H. K. *Inorg. Chem.* **1970**, *9*, 2644.
(23) Bottomley, L. A.; Kadish, K. M. *Inorg. Chem.* **1981**, *20*, 1348.

0020-1669/88/1327-1814$01.50/0

Table I. Oxidation Potentials for Ligand Anions and Their Complexes with Zinc(II) and Manganese(II) in Acetonitrile (0.1 M Tetraethylammonium Perchlorate)

ligand anion $(L^-)^a$	$E_{1/2}$,[b] V vs NHE					
	$L^-/L^\bullet$	$Zn^{II}L_3^-/Zn^{II}L_2(L^\bullet)$	$Mn^{II}L_3^-/Mn^{II}(^\bullet L)L_2$	(ΔE_{Zn-Mn})	$Fe^{III}L_3^-/Fe^{III}L_3$	$Mn^{II}(^\bullet L)L_2/Mn^{II}(^\bullet L)_2L^+$
$8\text{-}Q^-$	+0.21	+0.22	−0.06	0.28	−0.41	+0.97
$acac^-$	+0.55	+0.58	+0.18	0.40	−0.41	+1.20
AcO^-	+1.38	+1.41	+0.44[c]	0.97	−0.30	+1.41[c]
PA^-	+1.50	+1.54	+0.60	0.94		+1.59

[a] Key: $8\text{-}Q^-$, 8-quinolinolate; $acac^-$, acetylacetonate; AcO^-, acetate; PA^-, picolinate. [b] In aqueous solution at pH 0, E° Mn(III/II) = +1.51 V vs NHE and $E^\circ_{Fe(III/II)}$ = +0.77 V vs NHE; in MeCN, $E^{\circ\prime}_{Mn(III/II)} > +2.5$ V NHE and $E^{\circ\prime}_{Fe(III/II)}$ = +1.8 V vs NHE. [c] Poorly resolved cyclic voltammogram.

Mn(II)[20] and for the hydroxide and phenoxide complexes of manganese(II), iron(III), and cobalt(II) porphyrins.[24]

Experimental Section

Equipment. The electrochemical experiments were accomplished with a Bioanalytical Systems Model CV-27 voltammograph, a Houston Instruments Model 200 XY recorder and a 15-mL electrochemical cell that included a Bioanalytical Systems glassy-carbon inlay electrode (area 0.09 cm^2), a platinum-wire auxiliary electrode, and a Ag/AgCl reference electrode. The reference electrode was contained in a Pyrex tube with a soft-glass cracked tip, filled with aqueous tetramethylammonium chloride at a concentration to give a potential of 0.00 V vs SCE, and placed inside a luggin capillary.[25] The platinum-wire auxiliary electrode was placed inside a glass tube closed with a medium-porosity glass frit.

The UV–visible spectra were obtained with a Hewlett-Packard Model 8450A diode-array spectrophotometer. X-ray absorption spectra were collected for powdered samples spread on tape by use of beam line X-11 at the National Synchrotron Light Source at Brookhaven National Laboratory.

Reagents. The reagents for the investigations and syntheses were the highest purity commercially available and were used without further purification. $Mn(acac)_3$ (McKenzie) was recrystallized from benzene before use. Burdick and Jackson "distilled in glass" grade acetonitrile (MeCN) was used without further purification as the solvent for the electrochemical experiments. High-purity argon gas was used to dearate the solutions.

Preparation and Complexes. Several manganese complexes were prepared by conventional methods: $Mn(PA)_2(H_2O)_2$,[26] $MnPA_3 \cdot H_2O$,[26] $Na[Mn(DPA)_2]$,[26] Mn(DPA)(DPAH)(EtOH),[27] $Mn(8\text{-}Q)_3$,[27,28] $Mn(urea)_6(ClO_4)_3$,[29] $Mn(Me_2SO)_6(ClO_4)_3$,[30] $Mn(Ph_3PO)_4(ClO_4)_2$,[31] $Mn(bpy)_3(ClO_4)_2$,[32] $[Mn(bpy)_2(O)]_2(ClO_4)_3(H_2O)_4$,[33,34] $[Mn(bpyO_2)_3]_2(S_2O_8)_3(H_2O)_8$,[35] $[Mn(terpyO_3)_2(H_2O)_2](ClO_4)_2$,[36] $[Mn(phen)_2(O)]_2(ClO_4)_4(H_2O)_4$,[37] Mn(TPP)Cl,[38] $MnTPP(ClO_4)$,[39] $MnTPP \cdot 2CH_3OH$,[40] $Fe(8\text{-}Q)_3$,[41] and $Fe^{III}Cl_8TPP(ClO_4)$[42,43] (acacH = acetylacetone; PAH = picolinic acid; $DPAH_2$ = 2,6-pyridinedicarboxylic acid; 8-QH = 8-quinolinol; bpy = 2,2′-bipyridyl; $bpyO_2$ = 2,2′-bipyridyl 1,1′-dioxide; $terpyO_3$ = 2,2′,2″-terpyridine 1,1′,1″-trioxide; phen = 1,10-phenanthroline).

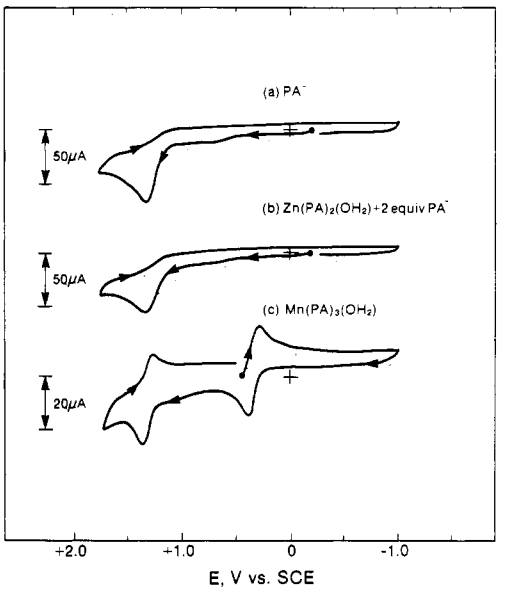

Figure 1. Cyclic voltammograms: (a) 3 mM picolinate (PA^-) [PAH + (TBA)OH, 1:1]; (b) 3 mM $Zn(PA)_2(H_2O)$ plus 2 equiv of PA^-; (c) 3 mM $Mn(PA)_3(OH_2)$ in MeCN (0.1 M tetraethylammonium perchlorate). Conditions: scan rate 0.1 V s^{-1}, 25 °C, glassy-carbon working electrode (0.09 cm^2), saturated calomel electrode (SCE) vs NHE, +0.242 V.

$Fe^{III}TPP(ClO_4)$. This tetraphenylporphinato (TPP) complex was prepared by a modification of the synthesis for (octaethylporphinato)-iron(III) perchlorate, with TPP used in place of OEP.[44]

$Zn(8\text{-}Q)_2 \cdot 2H_2O$. This complex was prepared by a modified procedure[45] that made use of $Zn(ClO_4)_2$ in place of $Zn(NO_3)_2$, where 0.5 equiv of $Zn(H_2O)_6(ClO_4)_2$ was added to an equimolar mixture of NaOH and 8-QH in water. The resulting yellow precipitate was collected on a glass frit, washed with ethanol, and dried in vacuo over $CaSO_4$. A similar synthesis was used for $Zn(PA)_2 \cdot 2H_2O$.

$(Me_4N)_2[Mn(PA)_2(O)]_2$. This complex was prepared by reacting $[Mn(bpy)_2(O)]_2(ClO_4)_3(H_2O)_2$ with 4 equiv of tetramethylammonium picolinate in acetonitrile to yield a dark brown precipitate.[46]

Mn(salpn)Cl. Addition of $Mn(OAc)_3 \cdot 2H_2O$ (2.68 g, 0.01 mol) and LiCl (0.63 g, 0.015 mol) to a solution of *N,N′*-disalicylidenepropanediamine (salpnH_2, 2.82 g, 0.01 mol) in methanol (100 mL) yielded a mixture that was refluxed for 1 h and then evaporated to dryness. The residue was washed with 2-propanol and then ether and dried in vacuo. The resulting product was recrystallized from MeCN. The Schiff-base ligand salpnH_2 was prepared by the condensation of salicylaldehyde and 1,3-propanediamine in ethanol. In a similar manner, the ligands salen (from 1,2-ethanediamine), *N*-hxsal (from *N*-hexylamine), and *N*-octsal (from *N*-octylamine) were formed and the complexes Mn(salen)Cl·H_2O, Mn(*N*-hxsal)$_2$Cl, and Mn(*N*-octsal)$_2$Cl prepared.[46]

$(Cl_8TPP)Mn(Cl)$. This porphinato complex was prepared by the addition of a 10-fold excess of $MnCl_2$ to a solution of 250 mg of tetrakis(2,6-dichlorophenyl)porphine (Cl_8TPPH_2) in 100 mL of DMF. The mixture was stirred and refluxed, with the extent of reaction monitored spectroscopically via the Cl_8TPPH_2 Soret band (λ_{max}, 416 nm). The

(24) Tsang, P. K. S.; Cofré, P.; Sawyer, D. T. *Inorg. Chem.* **1987**, *26*, 3604.
(25) Sawyer, D. T.; Roberts, J. L. Jr. *Experimental Electrochemistry for Chemists*; Wiley-Interscience: New York, 1974; p 144.
(26) Yamaguchi, K.; Sawyer, D. T. *Inorg. Chem.* **1985**, *24*, 971.
(27) Summers, J. Ph.D. Dissertation, University of Michigan, 1968; available from University Microfilms International, Ann Arbor, MI.
(28) Ray, M. M.; Adhya, J. N.; Biswas, D.; Poddar, S. N. *Aust. J. Chem.* **1966**, *19*, 1737.
(29) Aghabozorg, H.; Palenik, G. J.; Stoufer, R. C.; Summers, J. *Inorg. Chem.* **1982**, *21*, 3903.
(30) Prabhakaran, C. P.; Patel, C. C. *J. Inorg. Nucl. Chem.* **1968**, *30*, 867.
(31) Bannister, E.; Cotton, F. A. *J. Chem. Soc.* **1960**, 1878.
(32) Morrison, M. M.; Sawyer, D. T. *Inorg. Chem.* **1978**, *17*, 334.
(33) Nyholm, R. S.; Turco, A. *Chem. Ind. (London)* **1960**, 74.
(34) Plaksin, P. M.; Stoufer, R. C.; Mathew, M.; Palenik, G. J. *J. Am. Chem. Soc.* **1972**, *94*, 2121.
(35) Nyholm, R. S.; Turco, A. *J. Chem. Soc.* **1962**, 1121.
(36) Reiff, W. M.; Baker, W. A. *Inorg. Chem.* **1970**, *9*, 570.
(37) Goodwin, H. A.; Sylva, R. N. *Aust. J. Chem.* **1967**, *20*, 629.
(38) Ogoshi, H.; Wantanabe, E.; Yoshida, Z.; Kincaid, J.; Nakamoto, K. *J. Am. Chem. Soc.* **1973**, *95*, 2845.
(39) Hill, C. L.; Williamson, M. M. *Inorg. Chem.* **1985**, *24*, 2836.
(40) Camenzind, M. J.; Hollander, F. J.; Hill, C. L. *Inorg. Chem.* **1982**, *21*, 4301.
(41) Ohkaku, N.; Nakamoto, K. *Inorg. Chem.* **1971**, *10*, 798.
(42) Badger, G.; Jones, R. A.; Laslett, R. L. *Aust. J. Chem.* **1964**, *17*, 1028.
(43) Sugimoto, H.; Tung, H.-C., Sawyer, D. T. *J. Am. Chem. Soc.* **1988**, *110*, 2465.
(44) Dolphin, D. H.; Sams, J. R.; Tsin, T. B. *Inorg. Chem.* **1977**, *16*, 711.
(45) Charles, R. G. *J. Phys. Chem.* **1957**, *61*, 1640.
(46) Matsushita, T.; Spencer, L.; Sawyer, D. T. *Inorg. Chem.* **1988**, *27*, 1167.

Table II. Summary of Redox Potentials for Manganese and Iron Porphyrins in MeCN (0.1 M TEAP)

	$E_{1/2}$, V vs NHE			
	ring oxidns			
	$Mn^{II}(P^{2-})/Mn^{II}(\cdot P^{-})^{+}$	$Mn^{II}(\cdot P^{-})^{+}/Mn^{II}(P^{0})^{2+}$	$Mn^{II/III}$	axial ligand oxidn
Mn^{II}(TPP)	+0.06	+1.52	+1.75	
Mn(TPP)(ClO_4)	+0.04	+1.46	+1.75	
Mn(Cl_8TPP)(ClO_4)	+0.16	+1.73	*a*	
Mn(TPP)(OAc)	+0.04	*b*	*b*	+1.60
Mn(TPP)Cl	+0.06	*b*	*b*	+1.59
Mn(Cl_8TPP)Cl	+0.13	+1.70	*a*	+1.39

	$E_{1/2}$, V vs NHE		
	ring oxidns		
	1st	2nd	$Fe^{III/II}$
Fe^{III}(TPP)(ClO_4)	+1.35	+1.63	+0.35
Fe^{III}(Cl_8TPP)(ClO_4)	+1.58	+1.79	+0.44
Zn^{II}(TPP)	+0.99	+1.30	

[a] Oxidation is beyond the solvent window (>+2.0 V). [b] The large prewave prior to the axial ligand oxidation and the large peak current associated with axial ligand oxidation preclude observation of these oxidations.

Table III. Redox Chemistry of Manganese Complexes

I. Metal-Centered, Mn(III)/Mn(II)

aqueous media	$E^{o\prime}$, V vs NHE	complex in acetonitrile	$E^{o\prime}$,[a] V vs NHE
3 M $HClO_4$	+1.56	$[Mn^{II}(MeCN)_4]^{2+}$	>+2.54
7.5 M H_2SO_4	+1.49	$[Mn^{II}(DMU)_6]^{2+}$	+2.14
0.4 M $H_2P_2O_7^{2-}$ (pH 7.1)	+1.01	$[Mn^{II}(bpy)_3]^{2+}$	+1.61
		$[Mn^{II}(bpyO_2)_3]^{2+}$	+1.11
		$[Mn^{II}(tpyO_3)_2]^{2+}$	+1.30

II. Ligand-Centered, $Mn^{II}L_n/Mn^{II}(\cdot L)(L)_{n-1}$

aqueous media	E_{ox}, V vs NHE	complex in acetonitrile	E_{ox},[a] V vs NHE
0.1 M $N(CH_2CH_2OH)_3$ (pH 12)	−0.48	(i) $(HTDT^{-}/HTDT^{\cdot})$	+0.19
		$[Mn^{II}(TDT)_2]^{2-}$	−0.39
0.1 M gluconate (pH 13.5)	−0.03	$[Zn^{II}(TDT)_2]^{2-}$	+0.42
0.1 M catechol (pH 13.5)	−0.28	(ii) $(DTBCH^{-}/DTBCH^{\cdot})$	+0.12
MnO_4^{2-}/MnO_4^{-} (pH 14)	+0.56	$[Mn^{II}(DTBC)_2]^{2-}$	−0.27

[a] Based on anodic voltammograms. Key: TDT, 3,4-toluenedithiolate; DTBC, 3,5-*tert*-butylcatecholate; bpy, bipyridine; $bpyO_2$, bipyridine 1,1′-dioxide; $tpyO_3$, terpyridine 1,1′,1″-trioxide; DMU, dimethylurea.

mixture was allowed to cool and the solvent removed by rotary evaporation at 60 °C. After the solvent was removed, the excess $MnCl_2$ (oxidized) was removed by paper filtration of the solid mixture in CH_2Cl_2. The CH_2Cl_2 was then removed by rotary evaporation. (Cl_8TPP)Mn(ClO_4) was prepared by metathesis of (Cl_8TPP)Mn(Cl) with 0.99 equiv of anhydrous $AgClO_4$ in hot toluene and was recrystallized from hot toluene/heptane.[39]

Results

Electrochemistry. Figure 1 illustrates the cyclic voltammograms for picolinate anion (PA^{-}), $Zn^{II}(PA)_3^{-}$, and $Mn(PA)_3(H_2O)$. The latter is reversibly reduced to $Mn^{II}(PA)_3^{-}$ and reoxidized by two reversible one-electron steps (nominally attributable to the Mn(II)/Mn(III) and Mn(III)/Mn(IV) redox couples). The cyclic voltammograms for the 8-quinolinate, acetylacetonate, and acetate anions and their zinc and manganese complexes exhibit similar features. Although the ligand anions and zinc complexes exhibit irreversible oxidation peaks, the manganese complexes undergo two reversible oxidations. The $E_{1/2}$ values for these anions and their zinc and manganese complexes are summarized in Table I. The results for the acetate complex of manganese are anomalous. Instead of two reversible couples, the positive voltage scan yields broad, complex irreversible oxidation peaks (apparently due to the propensity of $Mn(OAc)_3(H_2O)$ to polymerize).

Figure 2 illustrates the cyclic voltammograms for ZnTPP, (TPP)Mn(ClO_4), and (TPP)Fe^{III}(ClO_4). The half-wave potentials ($E_{1/2}$) for the porphyrin complexes of zinc, manganese, and iron are summarized in Table II. Additional redox data are presented in Table III for various manganese complexes in aqueous and acetonitrile solutions and are grouped as metal-centered and ligand-centered processes.

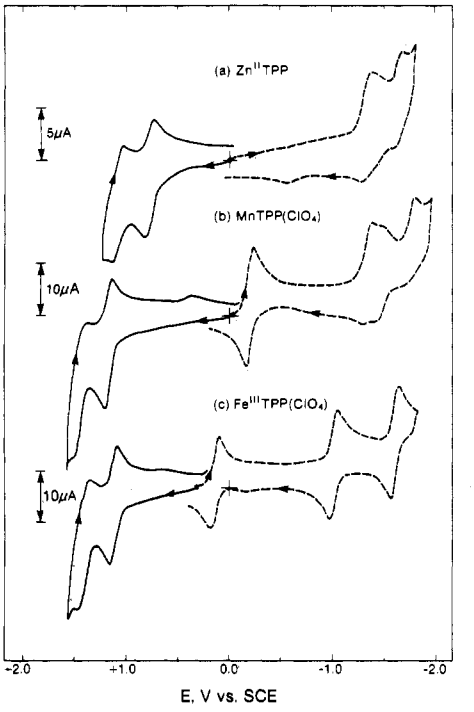

Figure 2. Cyclic voltammograms: (a) 0.66 mM Zn^{II}TPP, not completely soluble; (b) 0.61 mM MnTPP(ClO_4); (c) 0.52 mM Fe^{III}TPP(ClO_4) in MeCN (0.1 M tetraethylammonium perchlorate). Conditions: scan rate 0.1 V s^{-1}, glassy-carbon working electrode (0.07 cm^2), saturated calomel electrode (SCE) vs NHE, +0.242 V.

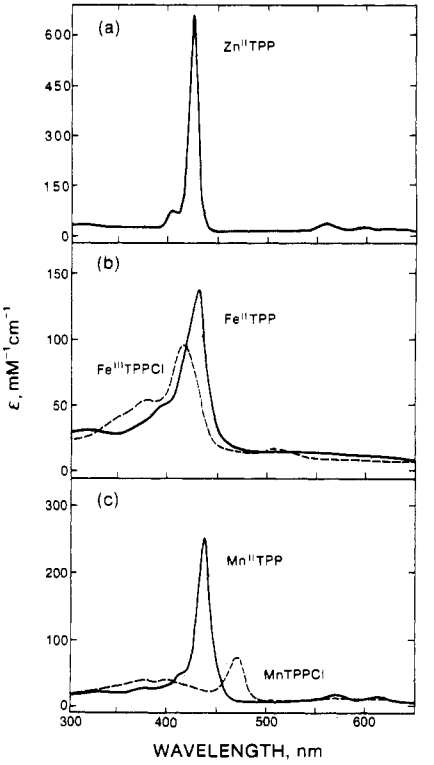

Figure 3. Absorption spectra: DMF for (a) 0.52 mM Zn^{II}TPP; (b) 0.58 mM Fe^{III}TPPCl and 0.58 mM Fe^{II}TPP; (c) 0.61 mM Mn(TPP)Cl and 0.61 mM Mn^{II}TPP.

Spectroscopy. Figure 3 illustrates the absorption spectra for Zn^{II}TPP, Fe^{III}(TPP)Cl, Fe^{II}TPP, (TPP)MnCl, and Mn^{II}TPP in dimethylformamide. The absorption spectra of electrochemically produced Mn^{II}TPP and Fe^{II}TPP are analogous to those that have been prepared by reduction with a 30-fold excess of $NaBH_4$.

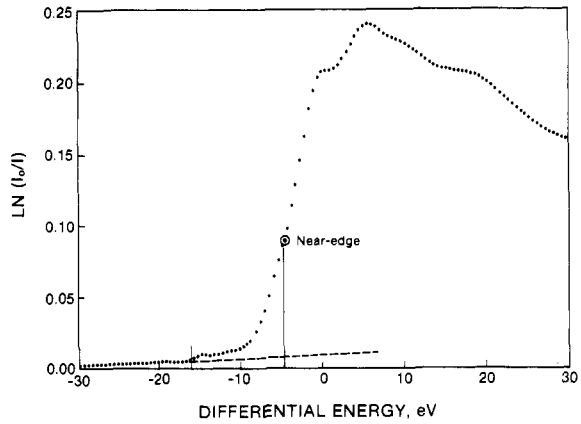

Figure 4. X-ray absorption spectrum for solid $Mn(PA)_3(OH_2)$. The reference energy, E_0, is the K-edge for manganese metal, 6537.4 eV.

X-ray Absorption Edges. The X-ray absorption spectrum for $Mn(8\text{-}Q)_3$ is shown in Figure 4, and indicates that the edge energies are taken at the inflection point of the absorption band. Table IV summarizes the near-edge energies for a series of solid-state (a) manganese(II) complexes, (b) their oxidized analogues (traditionally viewed as Mn(III) complexes), and (c) oxidized manganese–oxygen compounds (MnO_2 and $KMnO_4$). Both $[Mn_2(bpy)_4(\mu\text{-}O)_2](ClO_4)_3(H_2O)_2$ and MnO_2 exhibit shoulders along the major absorption edge; the edge values are for the first major inflection point.

Discussion and Conclusions

The oxidation potentials for the $Zn^{II}L_3^-$ complexes in Table I are slightly positive of those for the free ligand anions (L^-), which is due to the Lewis acidity interaction of Zn(II) with the ligand anion. Although Mn(II) has an acidity similar to that of Zn(II), the oxidation potentials for the $Mn^{II}L_3^-$ complexes are less positive by 0.28–0.97 V (Table I), and the oxidation processes are reversible (the oxidations of $Zn^{II}L_3^-$ and of L^- are irreversible). Also, a second reversible oxidation couple is observed for the $Mn^{II}L_3^-$ complexes. Although these couples traditionally are attributed to the Mn(II)/Mn(III) and Mn(III)/Mn(IV) metal-centered oxidation processes, the first [nominally Mn(II)/Mn(III)] occurs at a substantially less positive potential than (a) that for oxidation of solvated Mn(II) (in MeCN an oxidation peak is not observed before the solvent edge at +2.54 V vs NHE) or (b) that for oxidation of the free ligand anion. This negative shift in potential also has traditionally been rationalized as due to enhanced stabilization of high valence states. The trend of the oxidation potentials for the $Mn^{II}L_3^-$ complexes parallels that for the $Zn^{II}L_3^-$ complexes and the free L^- ligands. If stabilization of Mn(III) were the process, then the $Mn^{II}(PA)_2^-$ complex should have the least positive oxidation potential (instead, it has the most positive potential).

The shifts in the oxidation potentials for the $Mn^{II}L_3^-$ complexes are consistent with a ligand-centered oxidation. The ligand radical product ($^{\bullet}L$) is stabilized by covalent-bond formation with the d-electron manifold of the Mn(II) center. Manganese(II) is a high-spin d^5 center with the orbitals half-filled in a spherical array and available for bond formation via the unpaired p electron of an oxidized ligand radical. The stabilization that results from covalent-bond formation causes the oxidation potential to be less than that of the free anion. Therefore, the redox couple for the $[Mn^{II}(PA)_3]^-$ complex is best represented as the ligand-centered redox process $[Mn^{II}(PA)_3]^-/[Mn^{II}(^{\bullet}PA)(PA)_2]$. A comparison of the oxidation potentials for the $Zn^{II}L_3^-$ anions with the potentials for the first oxidation couple for the $Mn^{II}L_3^-$ complexes indicates a Mn(II)–L covalent bond strength of 7–23 kcal/mol [(0.3–1.0 V) × 23.1 kcal V^{-1}]. These values are in accord with the covalent bond strength (8 kcal) that has been observed for the hydroxide complex $Mn(OPPh_3)_4(OH)^+$.[24] The shifts in potential between the first redox couple and the oxidation peak of the free ligand anion parallel the ease of oxidation for the free ligand anions. The ligands with oxidizable carboxylate groups ($^-$OAc and PA^-) have the largest voltage shifts, which indicates that the Mn(II)–OC(O)R covalent bond is much stronger than the Mn(II)–OR bond. The second oxidation couple, $[Mn^{II}(^{\bullet}L)(L^-)_2/Mn^{II}(^{\bullet}L)_2(L^-)^+$, is approximately 1.0 V positive of that for the first couple, which is due the electrostatic effect of oxidizing a neutral complex rather than an anion.

The redox data of Table II for manganese porphyrins relative to that for iron and zinc porphyrins indicate that the oxidations of the $Mn^{II}(Por^{2-})$ complexes are ligand-centered. As in the case of manganese complexes of Table I and III, the ligand oxidation in $Mn^{II}(Por^{2-})$ is shifted to a much less positive potential than that in $Zn^{II}(Por^{2-})$. The shift of 0.93 V for the $Zn^{II}(TPP)/Mn^{II}(TPP)$ pair indicates a stabilization of 22 kcal mol^{-1} (0.93 V × 23.1 kcal V^{-1}) from the formation of a Mn(II)–($^{\bullet}Por^-$) covalent bond. This exceptional shift is reasonable, but unique, for the high-spin d^5-Mn(II) center of $Mn^{II}(Por^{2-})$ because removal an electron from the Por^{2-} ligand gives an unpaired p electron in the plane of the porphyrin. This electron will have a high degree of overlap (strong covalent bond) with the half-filled $d_{x^2-y^2}$ orbital of the Mn(II). In the case of ligand oxidation for $Fe^{III}(TPP)(ClO_4)$, the potential is more positive by 1.3 V because of the electrostatic effect [oxidation of $Fe^{III}(TPP)(ClO_4)$ rather than a neutral $Mn^{II}(TPP)$ complex (about −1.0 V from Table I)] and the absence of a half-filled $d_{x^2-y^2}$ orbital in the ground state of $Fe^{II}(TPP)(ClO_4)$ ($S = {}^3/_2$). The oxidation of $Mn^{II}(TPP)(OH)^-$ converts the $^-$OH ion to a covalently bound $^{\bullet}$OH group. The negative shift in oxidation potential from +0.92 V vs NHE for free $^-$OH to −0.16 V vs NHE for the hydroxide manganese porphyrin complex corresponds to the formation of a 25-kcal

Table IV. X-ray Absorption Edges for Solid Manganese Complexes and Compounds

	complex	major edge,[a] eV	assignts;[b] edge, eV
A	$Mn^{II}(OAc)_2(OH_2)$	6546.5	
	$Mn^{II}(PA)_2(OH_2)_2$	6546.5	
	$Mn^{II}(acac)_2$	6546.0	
	$[Mn^{II}(terpyO_3)_2](ClO_4)_2\cdot 2H_2O$	6546.0	
	$[Mn^{II}(bpy)_3](ClO_4)_2$	6546.0	
	$[Mn^{II}(OPPh_3)_4](ClO_4)_2$	6545.5	
	$Mn^{II}Cl_2$	6545.5	
			Mn(II); 6546 ± 0.3
B	$[Mn^{III}(bpyO_2)_3]_2(S_2O_8)_3\cdot 4H_2O$	6550.0	
			Mn(III); 6550 ± 0.5
C	MnF_3	6549.0	
	$Na_3[Mn(P_2O_7)_3]$	6549.0	
	$Mn(OAc)_3(OH_2)_2$	6549.0	
	$[Mn(urea)_6](ClO_4)_3$	6548.5	
	$[Mn(Me_2SO)_6](ClO_4)_3$	6548.5	
	$Mn(PA)_3(OH_2)$	6548.5	
	$Mn(acac)_3$	6548.5	
	Mn(salpn)Cl	6548.5	
	$Mn(salen)Cl\cdot H_2O$	6548.0	
	$Mn(8\text{-}Q)_3$	6548.0	
	$MnCl_3(phen)(OH_2)$	6548.0	
	Mn(TPP)(OAc)	6548.0	
	Mn(DPA)(DPAH)(EtOH)	6548.0	
	$(Bu_4N)[Mn(DPA)_2]$	6548.0	
			$Mn^{II}(^{\bullet}L)$; 6548.3 ± 0.5
D	$[Mn_2(bpy)_4(\mu\text{-}O)_2](ClO_4)_3\cdot 4H_2O$	6548.5	
	$[Mn_2(phen)_4(\mu\text{-}O)_2](ClO_4)_4\cdot 4H_2O$	6549.0	$Mn^{II}_2(O)_2$; 6549 ± 0.5
E	MnO_2	6551.0	$Mn^{II}(^{\bullet}O^-)_2$; 6551 ± 0.5
F	$KMnO_4$	6556.5	$Mn^{II}(O)(^{\bullet}O^-)_3^-$; 6556 ± 1.0

[a] Position of first major inflection point after Mn K-edge at 6537.4 eV; reproducibility, ±0.5 eV. [b] For $Co^{III}L_3$ and $Co^{II}L_2$, $\Delta E_{edge} = 4.0$ eV.[54]

covalent bond. This single-bond energy is consistent with the gas-phase double-bond energies for $(Mn-O)^+$ and Mn–O (double bonds, 57 kcal and 85 kcal, respectively).[47]

The conclusion that $Mn^{II}(Por^{2-})$ complexes are oxidized by a ligand-centered process is supported by the spectral data of Figure 3. The unsplit and intense Soret band for $Zn^{II}(TPP)$, which reflects the electron density of the porphyrin and the effect of the metal center on the electron density, indicates minimal interaction between metal d(π) and porphyrin ring (π) orbitals.[48] Whereas the absorption spectra for $Fe^{III}(TPP)Cl$, $Fe^{II}(TPP)$, and $Mn^{II}(TPP)$ have significant and intense Soret bands, those for the oxidized manganese porphyrin $[Mn(TPP)^+]$ and for $Zn^{II}(Por^{\bullet-})^+$[49] only have low-intensity bands in the Soret region (Figure 3). Others[50] have suggested that this absence of a strong Soret band indicates "...that Mn(III) is strongly perturbing the porphyrin π-system." We would agree and conclude that Mn(III) transfers an electron from the π-system to give $Mn(II)-(^{\bullet}Por^-)$. X-ray data[51,52] for Mn(TPP)Cl confirm that the Mn–N bond distances are short because of a strong metal–porphyrin interaction.[50] The present spectral and electrochemical data support this via the formation of a covalent bond between the d orbitals of Mn(II) and the π-manifold of the porphyrin radical to give $Mn^{II}(^{\bullet}Por^-)^+$ for oxidized manganese porphyrins.

This formulation is further supported by the independence of the reduction potential for the $Mn^{II}(^{\bullet}P^-)^+/Mn^{II}(P^{2-})$ couple from the presence of various axial ligands. In a metal-centered redox process the oxidation potential depends on the nature and presence of an axial ligand, as is observed for the $Fe^{III}(TPP)X$ complexes.[53] The axial ligand favors a neutral complex and adds electron density to the iron center, which stabilizes the higher oxidation state and makes removal of an electron less difficult. But in the case of a ligand-centered redox process such a shift is not expected and is not observed for the Mn(TPP)X complexes (Table II). If the formulation $[Mn^{II}(^{\bullet}P^-)]^+$ is assumed, then the d^5 configuration indicates the availability of an unpaired d-electron in the plane of the pyrrole nitrogens (i.e., $d_{x^2-y^2}$). This unpaired electron can then form a covalent bond with the unpaired p electron of the oxidized porphyrin to give a net spin of $S = {}^4/_2$ [traditionally formulated as d^4 Mn(III)]. Because this path of stabilization is available for Mn(II) porphyrins, the first ring oxidations of these species occur at much lower potentials than that of $Zn^{II}(TPP)$ (see Table II).

The oxidation potentials in MeCN for $Fe^{II}(MeCN)_4(ClO_4)_2$ (+1.85 V vs NHE) and $Mn^{II}(MeCN)_4(ClO_4)_2$ (>+2.54 V vs NHE; not observed within the solvent window) indicate the Fe(III)/Fe(II) couple should be about 0.8 V more negative than the Mn(III)/Mn(II) couple in metalloporphyrins. Thus, the formulation of $[Mn^{II}(^{\bullet}Por^-)]^+$ is consistent with this order, whereas the $Mn^{III}(Por^{2-})^+$ formulation would be in conflict.

The X-ray absorption edge data of Table IV can be categorized to be consistent with the interpretations of the electrochemical results. The edge energies for Mn(II) complexes are in the range 6545.5–6546.5 eV, while that for $[Mn^{III}(bpyO_2)_3](S_2O_8)_3(H_2O)_8$ is 6550 eV. The metal center of this complex is surrounded by oxidized ligands and is a d^4 Mn(III). Thus, the shift in edge energy with valence is about +4.0 eV per oxidation-state change (the shift for Co(II) to Co(III) also is +4 eV),[54] which is consistent with an edge energy of 6537.4 eV for zerovalent manganese metal. For organic-ligand complexes [traditionally formulated as $Mn^{III}(L^-)_3$], the average edge energy is 6548.3 eV (Table IV), which corresponds to an edge shift of +2.3 eV from the formation of a $Mn^{II}(^{\bullet}L)(L^-)_2$ covalent bond (indicated by the electrochemical results). The more ionic complexes with weak covalent bonds, like MnF_3, have slightly higher edge energies. The edge of 6548.5 eV for the Nyholm complex is consistent with a formulation, $[(bpy)_2Mn^{II}(\mu\text{-}^{\bullet}O^{\bullet})(\mu\text{-}^{\bullet}O^-)Mn^{II}(bpy)_2]^{3+}$, that averages one covalent bond per Mn(II).

In the case of the porphyrin the edge energy is consistent with a Mn(II) center covalently bound to a porphyrin radical, $Mn^{II}(^{\bullet}TPP^-)(^-OAc)$. The data for MnO_2 can be rationalized with a formulation of two covalent bonds to monovalent oxygen atoms, $Mn^{II}(^{\bullet}O^-)_2$; and for $KMnO_4$ five covalent bonds are indicated, $[Mn^{II}(^{\bullet}O^{\bullet})(O^{\bullet-})_3]^-$. As such it should have an estimated edge energy of 6557.5 ($5 \times 2.3 = 11.5$ eV shift); the observed energy is 6556.5 eV. The covalent bonds undoubtedly are weakened as the Mn center becomes congested with multiple covalent bonds.

The conclusion from the present results that the oxidation of Mn(II) complexes is ligand-centered almost certainly applies to all manganese complexes with organic ligands. Hence, the extensively studied catechol complexes[55] $[Mn^{IV}(DTBC)_3^{2-}$ and $Mn^{III}(DTBC)_2^-$ where DTBC = 3,5-di-*tert*-butylcatechol dianion] are more accurately formulated as $Mn^{II}(DTBSQ)_2(DTBC)^{2-}$ and $Mn^{II}(DTBSQ)(DTBC)^-$ with two and one ligands oxidized to semiquinone anion radicals, respectively. Likewise the polyol complexes[21] (glucomate and sorbital dianions) that have been formulated as $Mn^{IV}(L^{2-})_3^{2-}$ and $Mn^{III}(L^{2-})_2^-$ are more appropriately represented by the formulae $Mn^{II}(^{\bullet}L^-)_2(L^{2-})^{2-}$ and $Mn^{II}(^{\bullet}L^-)(L^{2-})^-$, respectively. The same modification is in order for the Mn(IV) and Mn(III) complexes with Schiff bases, EDTA, and phthalocyanine.[21]

Acknowledgment. This work was supported by the National Institutes of Health, USPHS, under Grant GM-36289 and the National Science Foundation under Grant CHE-8516247. Beam line X-11 of the National Synchrotron Light Source at Brookhaven National Laboratory is supported by the Division of Materials Science of DOE under Contract DE-AS05-80-ER10742. We are grateful (a) to Dr. T. Matsushita for samples of binuclear and Schiff-base manganese complexes, (b) to Drs. K. M. Barkigia, J. Fajer, A. Forman, L. Hanson, and M. W. Renner of Brookhaven National Laboratory (with the support of the Division of Chemical Sciences under Contract DE-AC02-76CH0016) for their collection of the X-ray absorption edge data, (c) to the National Science Foundation for the award of a Graduate Fellowship to S.A.R., and (d) to the U.S. Air Force Institute of Technology Civilian Institute Program for the award of a Fellowship to S.A.R.

Registry No. $8\text{-}Q^-$, 19314-53-5; $acac^-$, 17272-66-1; AcO^-, 71-50-1; PA^-, 3198-27-4; $HTDT^-$, 99923-32-7; $DTBCH^-$, 65767-25-1; $[Zn(8\text{-}Q)_3]^-$, 113859-67-9; $[Zn(acac)_3]^-$, 36443-24-0; $[Zn(AcO)_3]^-$, 46140-22-1; $[Zn(PA)_3]^-$, 108617-24-9; $[Mn(8\text{-}Q)_3]$, 61060-88-6; $[Mn(acac)_3]^-$, 71974-81-7; $[Mn(AcO)_3]^-$, 58636-19-4; $[Mn(PA)_3]^-$, 113859-68-0; $[Fe(8\text{-}Q)_3]^-$, 113859-69-1; $[Fe(acac)_3]^-$, 21534-23-6; $[Fe(AcO)_3]^-$, 113859-70-4; Mn(TPP), 31004-82-7; $Mn(TPP)(ClO_4)$, 67161-73-3; $Mn(Cl_8TPP)(ClO_4)$, 113859-71-5; Mn(TPP)(OAc), 58356-65-3; Mn(TPP)Cl, 32195-55-4; $Mn(Cl_8TPP)Cl$, 91463-17-1; $Fe(TPP)(ClO_4)$, 57715-43-2; $Fe(Cl_8TPP)(ClO_4)$, 113859-72-6; Zn(TPP), 14074-80-7; $[Mn(MeCN)_4]^{2+}$, 56841-03-3; $[Mn(DMU)_6]_2^{+}$, 45311-37-3; $[Mn(bpy)_3]^{2+}$, 21340-25-0; $[Mn(bpyO_2)_3]^{2+}$, 52760-53-9; $[Mn(tpyO_3)_2]^{2+}$, 64939-15-7; $[Mn(TDT)_2]^{2-}$, 94595-52-5; $[Zn(TDT)_2]^{2-}$, 99923-31-6; $[Mn(DTBC)_2]^{2-}$, 113859-73-7; $Mn(OAc)_2(OH_2)$, 113859-74-8; $Mn(PA)_2(OH_2)_2$, 32355-32-1; $Mn(acac)_2$, 14024-58-9; $[Mn(terpyO_3)_2](ClO_4)_2\cdot 2H_2O$, 113859-81-7; $[Mn(bpy)_3](ClO_4)_2$, 36578-61-7; $[Mn(OPPh_3)_4](ClO_4)_2$, 108985-78-0; $MnCl_2$, 7773-01-5; $[Mn(bpyO_2)_3]_2(S_2O_8)_3\cdot 4H_2O$, 113859-84-0; MnF_3, 7783-53-1; $Mn(OAc)_3(OH_2)_2$, 113859-75-9; $[Mn(urea)_6](ClO_4)_3$, 82823-06-1; $[Mn(Me_2SO)_6](ClO_4)_3$, 20703-10-0; $Mn(PA)_3(OH_2)$, 113859-76-0; $Mn(acac)_3$, 14284-89-0; Mn(salpn)Cl, 99568-94-2; $Mn(salen)Cl\cdot H_2O$, 53177-12-1; $Mn(8\text{-}Q)_3$, 14375-91-8; $MnCl_3(phen)(OH_2)$, 15613-08-8; Mn(DPA)(DPAH)(EtOH), 94859-42-4; $(Bu_4N)[Mn(DPA)_2]$, 113859-77-1; $[Mn_2(bpy)_4(\mu\text{-}O)_2](ClO_4)_3\cdot 4H_2O$, 113859-82-8; $[Mn_2(phen)_4(\mu\text{-}O)_2](ClO_4)_4\cdot 4H_2O$, 113859-78-2; MnO_2, 1313-13-9; $KMnO_4$, 7722-64-7; DMF, 68-12-2; MeCN, 75-05-8; Mn, 7439-96-5; C, 7440-44-0.

(47) Kang, H.; Beauchamp, J. L. *J. Am. Chem. Soc.* **1986**, *108*, 5663.
(48) Gouterman, M. *J. Chem. Phys.* **1959**, *30*, 1139.
(49) Felton, R. H. In *The Porphyrins*; Dolphin, D., Ed.; Academic: New York, 1978; Vol. V, Part C, pp 81–88.
(50) Boucher, L. J. *Coord. Chem. Rev.* **1972**, *7*, 289.
(51) Tulinsky, A.; Chen, B. M. L. *J. Am. Chem. Soc.* **1977**, *99*, 3647.
(52) Scheidt, W. R. In *The Porphyrins*; Dolphin, D., Ed.; Academic: New York, 1979; Vol. V, Part A, p 474.
(53) Kadish, K. M. In *Iron Porphyrins, Part II*; Lever, A. B. P., Gray, H. B., Eds.; Addison-Wesley: Reading, MA, 1983; pp 186–194.
(54) Srivasta, U. C.; Nigam, H. L. *Coord. Chem. Rev.* **1972**, *9*, 275.
(55) Chin, D.-H.; Sawyer, D. T.; Schaefer, W. P.; Simmons, C. J. *Inorg. Chem.* **1983**, *22*, 752.